Poly(ADP-ribose) polymerase gene disruption renders mice resistant to cerebral ischemia

MIKAEL J.L. ELIASSON[1,3], KENJI SAMPEI[5], ALLEN S. MANDIR[2], PATRICIA D. HURN[5], RICHARD J. TRAYSTMAN[5], JUN BAO[2], ANDREW PIEPER[3], ZHAO-QI WANG[6], TED M. DAWSON[2,3], SOLOMON H. SNYDER[1,3] & VALINA L. DAWSON[2-4]

[1]*Department of Pharmacology & Molecular Science,* [3]*Department of Neuroscience, and* [4]*Department of Physiology, Johns Hopkins University School of Medicine, 600 North Wolfe Street, Baltimore, Maryland 21205, USA*
[2]*Department of Neurology, Path 2-210, Johns Hopkins University School of Medicine, 600 North Wolfe Street, Baltimore, Maryland 21287, USA*
[5]*Anesthesiology and Critical Care Medicine, Johns Hopkins Medical Institutions, 600 North Wolfe Street, Baltimore, Maryland 21287, USA*
[6]*International Agency for Research on Cancer, 150, cours Albert Thomas, F-69008 Lyon, France*
Correspondence should be addressed to V.L.D.
e-mail valina_dawson@qmail.bs.jhu.edu

Nitric oxide (NO) and peroxynitrite, formed from NO and superoxide anion, have been implicated as mediators of neuronal damage following focal ischemia, but their molecular targets have not been defined. One candidate pathway is DNA damage leading to activation of the nuclear enzyme, poly(ADP-ribose) polymerase (PARP), which catalyzes attachment of ADP ribose units from NAD to nuclear proteins following DNA damage. Excessive activation of PARP can deplete NAD and ATP, which is consumed in regeneration of NAD, leading to cell death by energy depletion. We show that genetic disruption of PARP provides profound protection against glutamate-NO-mediated ischemic insults *in vitro* and major decreases in infarct volume after reversible middle cerebral artery occlusion. These results provide compelling evidence for a primary involvement of PARP activation in neuronal damage following focal ischemia and suggest that therapies designed towards inhibiting PARP may provide benefit in the treatment of cerebrovascular disease.

Poly(ADP-ribose) polymerase (PARP, EC 2.4.4.30) is a nuclear enzyme that utilizes NAD as a substrate to transfer up to 100 ADP-ribose groups to a variety of nuclear proteins, including histones as well as PARP itself, following its activation by DNA fragments[1-3]. The exact range of functions of PARP has not been established, although the enzyme is thought to play a role in DNA repair[2,4,5]. During major cellular stresses extreme activation of PARP may lead to cell death due to energy depletion[1]. Thus NAD, the substrate of PARP, is depleted by massive PARP activation, and in efforts to resynthesize NAD, ATP may also be depleted[1].

Neural damage following stroke and other neurodegenerative processes is thought to stem from overexcitation attributable to a massive release of the excitatory neurotransmitter glutamate acting on the *N*-methyl-D-aspartate (NMDA) receptor and other subtype receptors[6-8]. Evidence includes findings in many animal species that glutamate receptor antagonists block neural damage following vascular stroke and reduce neurotoxicity elicited by treatment of cerebral cortical cultures with glutamate or NMDA (ref. 9). Neurotoxicity elicited by stimulation of NMDA receptors is mediated, at least in part, by augmentation of nitric oxide (NO) formation, as NMDA receptor activation stimulates neuronal NO synthase (nNOS) activity. Protection against NMDA neurotoxicity occurs following treatment of primary brain cultures with NOS inhibitors[10,11] and in cortical cultures from mice with targeted disruption of nNOS (ref. 12). Neural damage following vascular stroke is markedly diminished in animals treated with NOS inhibitors[9,13] or in mice with nNOS gene disruption[14].

Nitric oxide is a free radical that chemically reacts with its cellular targets. There are multiple potential cellular targets that NO can modify to elicit a range of activities from cellular signaling to cell death. The majority of the toxic effects of NO appears to be a result of the reaction of NO with superoxide to form the very toxic compound peroxynitrite[12,15]. Both NO and peroxynitrite can cause DNA damage, which activates PARP (ref. 16–18). PARP activation plays a key role in NMDA- and NO-induced neurotoxicity, as PARP inhibitors prevent such toxicity in cortical cultures in proportion to their potencies as inhibitors of this enzyme[17].

Studies using drugs that are PARP inhibitors can be criticized on the grounds of lack of specificity and poor bioavailability. Recently Wang *et al.*[19] generated mice with targeted disruption of the gene that encodes PARP (*PARP*$^{-/-}$). Tissues from homozygous *PARP*-deleted mice display a loss of PARP catalytic activity. Although the mice are healthy and fertile and *PARP*$^{-/-}$ embryonic fibroblasts exhibit normal DNA excision repair, these mice display some abnormalities in cellular proliferation and are susceptible to the development of skin diseases with epidermal hyperplasia[19]. In the present study we demonstrate that cerebral cortical cultures from *PARP*$^{-/-}$ mice are completely resistant to neurotoxicity and that tissue damage following vascular stroke is profoundly reduced in *PARP*$^{-/-}$ animals.

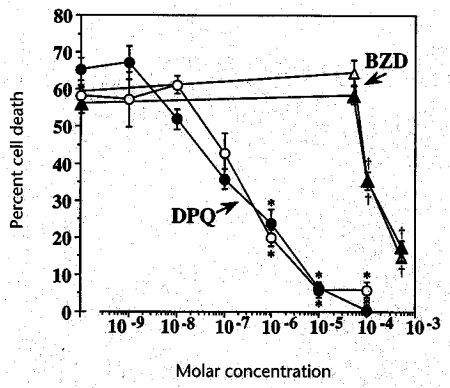

Fig. 1 PARP inhibitors attenuate *N*-methyl-D-aspartate (NMDA) and NO toxicity. The PARP inhibitors benzamide (BZD) (triangles) and 3,4-dihydro-5-[4-(1-piperidinyl) butox]-1(2H)-isoquinolinone (DPQ) (circles) inhibit toxicity induced by a 5-min exposure to 500 μM NMDA (open symbols) or 500 μM sodium nitroprusside (SNP) (closed symbols) neurotoxicity in a dose-dependent manner. DPQ is 500 times as potent as BZD and abolishes toxicity at maximal doses. Each data point is the mean ± s.e.m. ($n = 8$) of at least two separate experiments and reflects a minimum of 16,000 neurons counted. Significance was determined by a balanced two-way ANOVA demonstrating significance for the effects of DPQ ($F = 105$, $P \leq 0.0001$) and the Fisher PLSD *post hoc* test demonstrating differences at $^*P \leq 0.0001$ when comparing NMDA treatment with NMDA + DPQ or comparing SNP treatment with SNP + DPQ. A balanced two-way ANOVA demonstrating significance for the effects of BZD ($F = 178.42$, $P \leq 0.0001$) and the Fisher PLSD *post hoc* test differences were determined at $^\dagger P \leq 0.0001$ when comparing NMDA treatment with NMDA + BZD or comparing SNP treatment with SNP + BZD.

Neurotoxicity in cerebral cortical cultures is reduced in *PARP*$^{-/-}$ mice

Earlier we showed that the nonselective PARP inhibitors, such as benzamide and 3-aminobenzamide, reduce NMDA toxicity in cortical cultures and also reduce toxicity elicited by NO donors[17]. Benzamide and its derivatives are relatively weak PARP inhibitors with poor bioavailability. At a concentration of 100 μM, benzamide only provides a 50% protection against NMDA neurotoxicity[17]. More recently 3,4-dihydro-5-[4-(1-piperidinyl) butox]-1(2H)-isoquinolinone (DPQ) has been reported to be a much more potent and selective inhibitor of PARP with a 50% inhibitory concentration (IC_{50}) of 40 nM (ref. 20). Accordingly, we compared the effects of DPQ and benzamide in cortical cultures treated with NMDA or an NO donor, sodium nitroprusside (SNP) (Fig. 1). As reported previously, benzamide provides protection against NMDA- or NO-induced neurotoxicity with a median effective concentration (EC_{50}) of about 100 μM. By contrast, DPQ is much more potent providing 50% of maximal protection at 0.2 μM. At concentrations of 10–100 μM, DPQ virtually abolishes neurotoxicity, whereas the maximally effective concentration of benzamide only reduces neurotoxicity by 65%. The IC_{50} of benzamide for PARP is 22 μM (ref. 21, 22). Therefore, benzamide is a less potent inhibitor of PARP than DPQ; the difference is a factor of 500, which corresponds to the 500-fold difference in potencies of the compounds in protecting against neurotoxicity, fitting with the notion that PARP activation plays a role in neurotoxicity.

We next evaluated toxicity in cortical cultures elicited by NMDA or NO donors or by 60 min of oxygen and glucose deprivation (OGD), comparing cultures from wild-type and *PARP*$^{-/-}$ mice (Fig. 2). In wild-type cultures, NMDA kills approximately 65% of cells, consistent with previous observations[12]. NMDA-induced neurotoxicity is virtually abolished in cultures from *PARP*$^{-/-}$ animals and is not significantly different from buffer-treated controls, whereas in heterozygotes (*PARP*$^{+/-}$) toxicity is reduced by 72% (Fig. 2a). The NMDA antagonist MK801 abolishes NMDA toxicity in wild-type and heterozygote cultures, but has no effect on the minimal residual toxicity of *PARP*$^{-/-}$ cultures.

As NO has been shown to mediate the neurotoxic actions of NMDA (ref. 10–12), we evaluated the influence of the NO synthase (NOS) inhibitor nitroarginine on NMDA toxicity. Nitroarginine markedly reduces NMDA toxicity in wild-type cultures and the *PARP*$^{+/-}$ cultures. Arginine reverses the protective effect of nitroarginine, as previously reported[10–12], but has no significant effect in *PARP*$^{-/-}$ cultures. Neurotoxicity induced by the NO donor, sodium nitroprusside (SNP), is reduced by 73% in *PARP*$^{+/-}$ cultures and abolished in *PARP*$^{-/-}$ cultures. The *PARP*$^{-/-}$ cultures are also resistant to NO neurotoxicity induced by another NO donor, 3-morpholino-sydnonimine hydrochloride (SIN-1). These observations are consistent with the notion that PARP involvement in toxicity is distal to NOS.

We also examined the influence of PARP inhibitors on NMDA neurotoxicity. Benzamide (500 μM) reduces NMDA toxicity in wild-type cultures and *PARP*$^{+/-}$, with no significant effect on the negligible residual toxicity of *PARP*$^{-/-}$ preparations. DPQ (10 μM) produces greater reduction of NMDA toxicity than benzamide in wild-type and in *PARP*$^{+/-}$ cultures with no significant effects on *PARP*$^{-/-}$ preparations. DPQ also reduces toxicity elicited by the NO donor, SNP, in both wild-type and *PARP*$^{+/-}$ cultures with no effect on the *PARP*$^{-/-}$ cultures. These observations confirm the role of PARP in NMDA-mediated toxicity and demonstrate that the residual toxicity observed in the *PARP*$^{+/-}$ cultures is due to PARP activity.

The neurotoxicity in cortical cultures elicited by oxygen-glucose deprivation (OGD) has previously been shown to involve NMDA receptor and nNOS activation[12]. In *PARP*$^{-/-}$ cultures OGD toxicity is virtually abolished and is not significantly different from residual toxicity in buffer-treated control cultures (Fig. 2*b*). In wild-type cultures and *PARP*$^{+/-}$ cultures, MK801 and nitroarginine also reduce toxicity with no differential effects in *PARP*$^{-/-}$ preparations. L-Arginine reverses the nitroarginine protection in wild-type and *PARP*$^{+/-}$ culture preparations but not in *PARP*$^{-/-}$ cultures. Benzamide reduces OGD toxicity in wild-type and *PARP*$^{+/-}$ cultures preparations to the same extent that it diminishes NMDA toxicity with no influence on *PARP*$^{-/-}$ preparations. DPQ also abolishes OGD toxicity as it does for NMDA toxicity.

Neural damage after vascular stroke is reduced in *PARP*$^{-/-}$ mice

The combination of oxygen-glucose deprivation and NMDA neurotoxicity in primary neuronal cultures is a common *in vitro* model for studying early mechanisms of vascular stroke damage. Because of the profound neuroprotection against OGD and NMDA neurotoxicity in this model, we evaluated the extent of brain injury following middle cerebral artery occlusion (MCAo) in the transgenic *PARP*$^{+/-}$ and *PARP*$^{-/-}$ mice compared with that in wild-type mice (129/SV). Mice were subjected to 2 hours of MCAo followed by 22 hours of reperfusion, after which the extent of infarct was determined. Infarct volume is reduced by ~80% in *PARP*$^{-/-}$ animals compared with wild-type animals, 15.4 mm^3 versus 69.0 mm^3 (Fig. 3*a*). Significant decreases in injury are evident in each of the five coronal sections except in the most anterior 2 mm (Fig. 3*b*). Infarct volume in *PARP*$^{+/-}$ animals is also reduced by ~65% compared with that in wild-type animals,

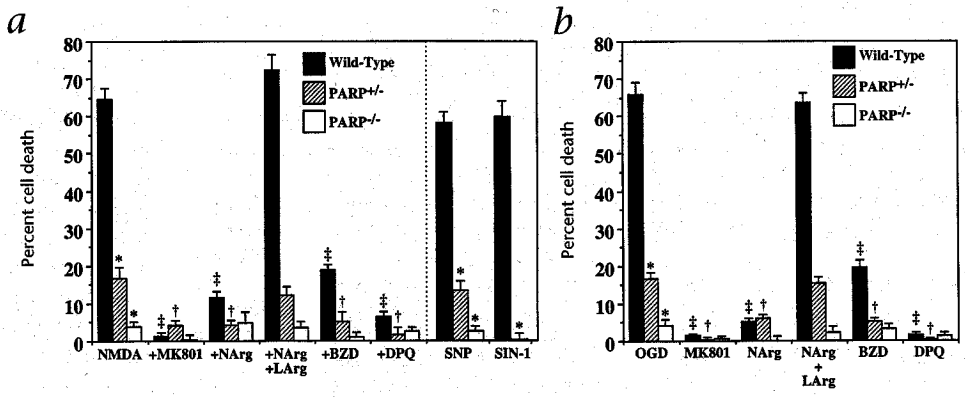

Fig. 2 Neurotoxicity is profoundly reduced in *PARP*$^{-/-}$ cerebral cortical cultures. *a*, A 5-min exposure to 500 μM NMDA kills approximately 65% and 17% of cells in wild-type and *PARP*$^{+/-}$, respectively. Toxicity in cultures from *PARP*$^{-/-}$ animals exposed to 500 μM NMDA is not significantly different from that in buffer-treated controls. The NMDA antagonist, MK801 (10 μM) abolishes NMDA toxicity in wild-type and heterozygote cultures. Nitroarginine (NArg) (100 μM), a selective inhibitor of NOS, reduces NMDA toxicity in wild-type cultures and the *PARP*$^{+/-}$ cultures. L-Arginine (LArg) (1 mM) reverses the protection against NMDA toxicity provided by NArg. Benzamide (BZD) (500 μM) reduces NMDA toxicity in wild-type and *PARP*$^{+/-}$ cultures. DPQ (10 μM) produces greater reduction of NMDA toxicity than benzamide in wild-type and in *PARP*$^{+/-}$ cultures. Neurotoxicity induced by the NO donor, sodium nitroprusside (SNP) (500 μM), is markedly reduced by 73% in *PARP*$^{+/-}$ cultures and abolished in *PARP*$^{-/-}$ cultures. The *PARP*$^{-/-}$ cultures are also resistant to NO neurotoxicity induced by the NO donor, 3-morpholino-sydnonimine hydrochloride (SIN-1) (1 mM). *b*, 60 min of oxygen-glucose deprivation (OGD) results in 65% cell death in wild-type cortical cultures, which is reduced to 15% in *PARP*$^{+/-}$. In *PARP*$^{-/-}$ cultures OGD toxicity is virtually abolished and is not significantly different from residual toxicity in buffer-treated control cultures. MK801 (10 μM) and NArg (100 μM) profoundly reduce toxicity in wild-type cultures and *PARP*$^{+/-}$ cultures. L-Arginine (1 mM) reverses the protection provided by NArg in wild-type and *PARP*$^{+/-}$ cultures. Benzamide (500 μM) reduces OGD toxicity and DPQ (10 μM) abolishes OGD toxicity in wild-type and *PARP*$^{+/-}$ cultures.

Each data point is the mean ± s.e.m. (n = 8) of at least two separate experiments. Each data point reflects a minimum of 16,000 neurons counted. Significance was determined by a balanced two-way ANOVA demonstrating significance for the effects of NMDA exposure on genotype ($F = 96.359$, $P \leq 0.0001$) or treatment ($F = 18.931$, $P \leq 0.0001$); or OGD on genotype ($F = 406$, $P \leq 0.0001$) or treatment ($F = 191$, $P \leq 0.0001$) and the Fisher PLSD *post hoc* test demonstrating differences at $^*P \leq 0.0001$ when comparing NMDA, SNP, SIN-1-treated or OGD-treated wild-type cultures with *PARP*$^{+/-}$ and *PARP*$^{-/-}$ cultures (genotype). The Fisher PLSD *post hoc* test demonstrated differences at $\ddagger P \leq 0.0001$ when comparing wild-type NMDA-treated or OGD-treated cultures with cultures with the addition of MK801, NArg, BZD or DPQ and differences at $\dagger P \leq 0.0001$ when comparing NMDA-treated cultures from *PARP*$^{+/-}$ animals with MK801, NArg, BZD or DPQ treatments in the *PARP*$^{+/-}$ cultures (treatment).

30.1 mm^3 versus 69.0 mm^3 (Fig. 3*a*) with significant protection in the three most caudal sections (Fig. 3*b*).

In two of the *PARP*$^{-/-}$ animals negligible infarct volume was observed, and these animals displayed no neurologic deficit at 22 hours of reperfusion. It is conceivable that these two mice have been completely protected against stroke damage. Alternatively, in these two animals the filament may not have been optimally placed to elicit MCAo. Because of the lack of neurologic deficit at 22 hours, data from these two mice have not been included in analyses of infarct volume (Fig. 3). If data from these two mice were included, the overall infarct volume for the *PARP*$^{-/-}$ group would be decreased from 15.4 mm^3 ± 1.8 to 12.1 mm^3 ± 1.6 ($n = 10$).

Hemodynamic measures are unaltered in *PARP*$^{-/-}$ mice

Hemodynamic alterations can markedly influence the effects of vascular stroke. Accordingly, physiology was monitored in wild-type, *PARP*$^{+/-}$ and *PARP*$^{-/-}$ animals before, during and after MCAo (Table 1). Regional cerebral blood flow (rCBF) is decreased to approximately 30% of baseline following MCAo and sustained during 2 hours of ischemia similarly among all three groups (Fig. 4). After removal of the filament, rCBF immediately increases to 90–110% of baseline. There are no significant differences in mean arterial blood pressure, core temperature, or blood gases between the groups that could provide nonspecific neuroprotection. Thus, reduction of infarct volume in the *PARP*$^{+/-}$ and *PARP*$^{-/-}$ animals does not result from altered hemodynamic effects on cerebral blood flow, body temperature, blood gases or blood pressure.

PARP protein and catalytic activity are undetectable Because of the pronounced reduction in neurotoxicity and stroke damage in *PARP*$^{+/-}$ as well as in *PARP*$^{-/-}$ mice, we compared PARP protein expression and catalytic activity in the adult mouse forebrain (Fig. 5). Wang and colleagues[19,23] demonstrated abolition of PARP protein and catalytic activity in cultured embryonic fibroblasts from *PARP*$^{-/-}$ mice but did not report data from *PARP*$^{+/-}$ mice. PARP activity is much higher in embryonic and postnatal tissue than in adult tissues, so that PARP protein and catalytic activity are not readily detectable in adult mice.

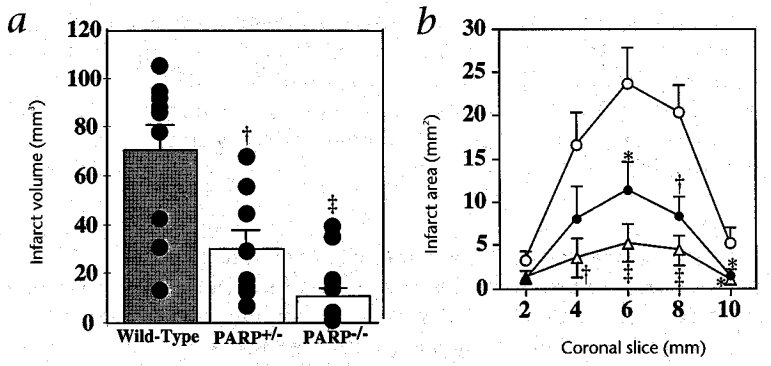

Fig. 3 Protection against focal ischemia in PARP-deficient mice. Infarct volume (*a*) and area (*b*) after transient focal ischemia in wild-type (○), *PARP*$^{+/-}$ (●) and *PARP*$^{-/-}$ (△) mice. Animals were subjected to MCA filament occlusion for 2 h and reperfused for 22 h as described. The forebrains were sliced into five coronal sections, 2 mm thick, and stained with 1% 2,3,5-triphenyltetrazolium chloride. The volume of infarction was determined by numeric integration of areas of marked pallor with section thickness. Data are presented as the means ± s.e.m. (Control, $n = 9$; *PARP*$^{+/-}$, $n = 8$; *PARP*$^{-/-}$, $n = 8$). Significance was determined by comparing *PARP*$^{+/-}$ or *PARP*$^{-/-}$ to wild-type by using a one-way ANOVA with Fisher's *post hoc* test. $^*P \leq 0.05$; $\dagger P \leq 0.01$; $\ddagger P \leq 0.001$. Additionally, a data point from each individual animal is plotted as a separate point overlayed on each histogram bar.

Table 1 Physiological variables before, during, and after middle cerebral artery occlusion in wild-type (129/SV), *PARP*$^{+/-}$ or *PARP*$^{-/-}$ mice under halothane anesthesia

Parameters	*Animal*	*Before*	*During*	*After*
MABP (mmHg)	Wild type	86 ± 4	85 ± 5	79 ± 5
	PARP$^{+/-}$	89 ± 9	86 ± 9	76 ± 4
	PARP$^{-/-}$	81 ± 8	81 ± 5	78 ± 6
Core temperature (°C)	Wild type	35.7 ± 0.5	35.9 ± 0.4	35.7 ± 0.5
	PARP$^{+/-}$	35.7 ± 0.5	36.0 ± 0.6	35.9 ± 0.6
	PARP$^{-/-}$	36.0 ± 0.4	36.2 ± 0.4	36.1 ± 0.8
Arterial pH	Wild type	7.27 ± 0.02	7.27 ± 0.02	
	PARP$^{+/-}$	7.28 ± 0.01	7.28 ± 0.00	
	PARP$^{-/-}$	7.27 ± 0.02	7.27 ± 0.01	
Arterial $PaCO_2$ (torr)	Wild type	41 ± 6	40 ± 1	
	PARP$^{+/-}$	37 ± 3	39 ± 3	
	PARP$^{-/-}$	38 ± 3	38 ± 1	
Arterial PaO_2 (torr)	Wild type	145 ± 12	136 ± 10	
	PARP$^{+/-}$	141 ± 8	120 ± 20	
	PARP$^{-/-}$	126 ± 34	116 ± 22	

MABP (mean arterial blood pressure), core temperature, and arterial blood gases (pH, $PaCO_2$, PaO_2) were measured before occlusion, during ischemia (2 h), and during up to 30 min of reperfusion. Data are presented as the means ± s.d. (wild type, $n = 4$; *PARP*$^{+/-}$, $n = 3$; *PARP*$^{-/-}$, $n = 3$). Values were averaged over 15 min before, 2 h during, and 1 h following middle cerebral artery occlusion.

Nevertheless we successfully identified PARP protein and catalytic activity, detectable at modest levels in wild-type mouse forebrain (Fig. 5). PARP protein expression is markedly reduced from wild-type in the *PARP*$^{+/-}$ forebrain and is not detectable in the *PARP*$^{-/-}$ forebrain (Fig. 5*a*). PARP catalytic activity is not detectable in the forebrain from *PARP*$^{+/-}$ or *PARP*$^{-/-}$ mice. We estimate that our PARP assays should have detected as little as 20% of wild-type activity, so that enzyme activity is probably reduced by at least 80% in the *PARP*$^{+/-}$ mice despite a lesser depletion of PARP protein.

ADP-ribose polymer formation is absent in *PARP*$^{-/-}$ cortex

ADP-ribose polymer formation is a marker of PARP catalytic activity. Wild-type mice express high levels of nuclear ADP-ribose polymer formation as identified by immunohistochemistry in the ipsilateral cortex following 2 hours of MCAo and 2 hours of reperfusion (Fig. 6, *a* and *b*). There is minimal nuclear staining in the contralateral hemisphere of the same animal. In both the ipsilateral and contralateral cortical hemispheres in the *PARP*$^{-/-}$ animals following 2 hours of MCAo and 2 hours of reperfusion there is a complete absence of any ADP-ribose polymer staining (Fig. 6, *c* and *d*).

Discussion

The major finding of this study is the dramatic protection observed in *PARP*$^{-/-}$ animals against ischemia. In cortical cultures ischemic damage is virtually abolished in neurons derived from *PARP*$^{-/-}$ animals. NMDA neurotoxicity has been examined in other mice with genetic alterations. In nNOS$^{-/-}$ mice[12] and in transgenic mice overexpressing copper-zinc superoxide dismutase[24], only about 50–60% maximal protection against NMDA toxicity is observed in the same culture systems as those utilized in the present study. Protection against vascular damage following middle cerebral artery occlusion is also impressive. The 80% reduction in infarct volume of *PARP*$^{-/-}$ mice exceeds protection reported with any known treatment. Maximal protection of 50–65% typically occurs with glutamate receptor antagonists[7,25], NOS inhibitors[9,26], treatment with the immunosuppressant FK506 (ref. 27) and after genetic alterations such as in transgenic nNOS$^{-/-}$ mice[14] and mice overexpressing copper-zinc superoxide dismutase[28,29]. Independently, Moskowitz and associates[30] have also observed pronounced protection against vascular stroke damage in *PARP*$^{-/-}$ animals. The profound neuroprotection observed in the *PARP*$^{-/-}$ mice, which exceeds protection reported for any other transgenic model or pharmacologic treatment, may represent a common role for PARP activation by other excitotoxic mechanisms in addition to production of free radicals and NO. Additionally, the failure of reported pharmacologic approaches to provide the dramatic protection conferred by the disruption of the *PARP* gene may reflect issues of bioavailability and drug delivery.

Recently the genetic variation among 129 substrains of mice was reported[31]. Because of the genetic variance between the 129-derived embryonic stem cell lines used for the construction of transgenic animals and the 129 mice available for experimental studies, we cannot exclude the possibility that the dramatic protection we observe in the *PARP*$^{-/-}$ mice is due to a cosegregating gene from the 129-derived embryonic stem cells. However, reported genetic variability in response to stroke damage between inbred lines of mice is at most 10% (ref. 14). Additionally, we have not observed variability in tissue cultures between strains of mice *in vitro* in response to NMDA- or NO-mediated neurotoxicity in this or other studies[12]. We routinely use a strain of related 129 mice in our control experiments. Our observations *in vitro* and *in vivo* argue against a genetic contribution by the 129-derived embryonic stem cell line in our models of glutamate neurotoxicity and focal ischemia.

The reduction in stroke damage in *PARP*$^{-/-}$ animals suggests that PARP inhibitors will be useful for treating strokes. This notion is supported by the pronounced protection against NMDA and OGD neurotoxicity afforded by the selective PARP inhibitor DPQ. Greenberg and colleagues[32] have demonstrated that DPQ provides marked protection against neural damage following

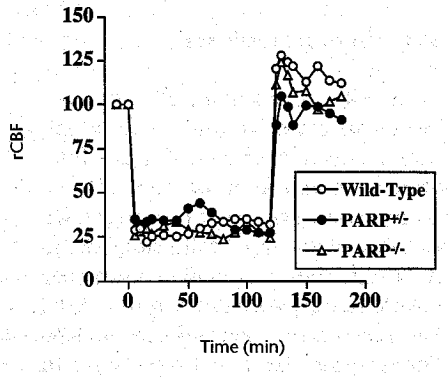

Fig. 4 Regional cerebral blood flow before, during and after 2 h of middle cerebral artery occlusion. The laser-doppler probe was placed on the skull ipsilateral to the occlusion: 2 mm posterior and 3 mm lateral from the bregma. Wild-type ($n = 4$), *PARP*$^{+/-}$ ($n = 3$), or *PARP*$^{-/-}$ ($n = 3$) mice. Data were analyzed by a one-way ANOVA with Fisher's *post hoc* test. There were no significant differences between the groups. The standard deviations are not shown for clarity, but the mean of the standard deviations for each data point is 8.2. Abbreviations: rCBF, regional cerebral blood flow.

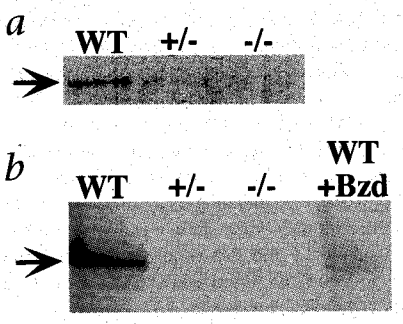

Fig. 5 PARP expression and catalytic activity are reduced in *PARP*-deficient mice. PARP expression (*a*) and catalytic activity (*b*) in the mouse brain is markedly reduced in the $PARP^{+/-}$ and $PARP^{-/-}$ mouse brains as compared with wild-type (WT). Protein expression was determined by western blot analysis, and catalytic activity was determined by a self-modification assay. Arrows denote the expression of PARP protein (*a*) or PARP catalytic activity (*b*). In the wild-type catalytic assay other ribosylated nuclear proteins present as the grey background, which is reduced with benzamide treatment (WT + Bzd) and is absent in the $PARP^{+/-}$ (+/–) and $PARP^{-/-}$ (–/–) lanes confirming the reduced expression and absence of PARP protein in the brains of these animals. Data shown are representative of duplicate experiments.

vascular stroke in rats.

Reduction in stroke damage and neurotoxicity in $PARP^{+/-}$ mice is almost as great as in $PARP^{-/-}$ mice. This protection parallels the greater than 80% reduction in enzyme activity in the $PARP^{+/-}$ preparations. The marked reduction in PARP expression in $PARP^{+/-}$ mice suggests that more than gene copy number affects the expression of PARP in adult brain. Since PARP is involved in regulating the normal activity of numerous nuclear proteins[2], it is possible that the loss of one *PARP* allele significantly affects transcriptional elements that regulate the mature expression of PARP, resulting in lower than expected protein expression.

Activation of PARP may also be important in conditions other than neurotoxicity. For instance, cytokine and oxidant damage to pancreatic islet cells and hepatocytes is reversed by PARP inhibitors[16,33] and in $PARP^{-/-}$ mice[34]. PARP inhibitors block cardiac damage following occlusion of coronary arteries[35]. Peroxynitrite toxicity to pulmonary epithelium, macrophages and smooth muscle cells is also blocked by PARP inhibitors[36–41]. Accordingly, PARP inhibitors may be therapeutic in a variety of nonneurologic conditions such as myocardial infarction.

Earlier studies had suggested that PARP activation following DNA damage may be one of several factors contributing to cell death in cerebral ischemia. Consistent with this notion are our observations that ADP-ribose polymer formation is induced in ischemic tissue but not in the contralateral, nonischemic hemisphere of the same animal. Additionally, there is complete absence of ADP-ribose formation in the $PARP^{-/-}$ following MCAo. The present study indicates that PARP activation may be a principal determinant of cell death. In neurotoxicity the following sequence of events presumably takes place (Fig. 7). Ischemia following blood vessel occlusion reduces the resting membrane potential of glia and neurons in the brain. Potassium leaks out of cells and depolarizes neurons leading to a massive release of glutamate. Acting via NMDA receptors, glutamate triggers a release of NO, which combines with superoxide to form peroxynitrite. Peroxynitrite damages DNA and its fragments activate PARP. Massive activation of PARP depletes NAD via ADP-ribose polymer formation. ATP is depleted in an effort to resynthesize NAD leading to cell death by energy depletion. Inhibition of PARP activity spares the cell from energy loss, preventing irreversible depolarization of the neurons and thus provides neuroprotection.

Methods

Primary cortical cultures. Primary cortical cell cultures were prepared from gestational day 16 fetal mice in a procedure modified from that previously described[12]. Briefly, the cortex was dissected, and the cells were dissociated by trituration in modified Eagle's medium (MEM), 20% horse serum, 25 mM glucose and 2 mM L-glutamine following a 30-min digestion in 0.027% trypsin/saline solution (Gibco BRL, Gaithersburg, MD). The cells are plated on 15-mm multiwell plates coated with polyornithine. Four days after plating, the cells are treated with 5-fluoro-2-deoxyuridine for 3 days to inhibit proliferation of nonneuronal cells. Cells are then maintained in MEM, 10% horse serum, 25 mM glucose and 2 mM L-glutamine in a 8% CO_2 humidified 37 °C incubator. The growth medium is refreshed twice per week and the neurons are allowed to mature for 14 days in culture before being used for experiments. Ontogeny studies in wild-type cultures have shown that nNOS is expressed at mature levels by day 14 in culture. Mature levels of nNOS neurons correspond to 1–2% of total neuronal population[42,43].

Cytotoxicity. The cells were exposed to neurotoxic conditions as previously described[12]. Before exposure, the cells were washed with Tris-buffered control salt solution (CSS) containing 120 mM NaCl, 5.4 mM KCl, 1.8 mM $CaCl_2$, 25 mM Tris-HCl (pH 7.4) and 15 mM glucose. The exposure solutions containing experimental reagents were administered for 5 min and then washed off. The cells were then placed in growth medium and returned to the incubator overnight.

Combined oxygen-glucose deprivation was performed as previously described[44,45]. The culture medium was completely exchanged with deoxygenated, glucose-free Earle's balanced salt solution (EBSS) containing 116 mM NaCl, 5.4 mM KCl, 0.8 mM $MgSO_4$, 1 mM NaH_2PO_4 and 0.9 mM $CaCl_2$, bubbled with 5% H_2/85% N_2/5% CO_2. The cultures were kept in an

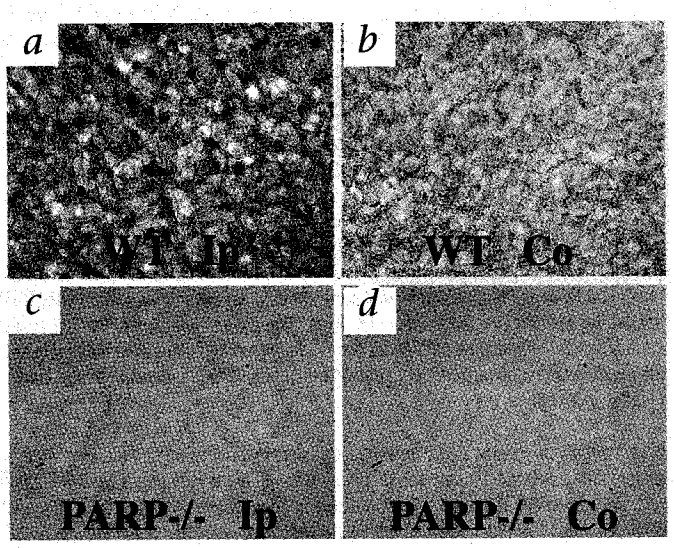

Fig. 6 ADP-ribose polymer formation is absent in the $PARP^{-/-}$ cortex following MCAo. Following 2 h of MCAo and 2 h reperfusion, ADP-ribose polymer formation is elevated in the nuclei in the ipsilateral cortex of wild-type mice (*a*) but not in the contralateral cortex (*b*). In the $PARP^{-/-}$ mice, neither the ipsilateral (*c*) or contralateral (*d*) cortex demonstrates any positive staining for ADP-ribose polymer. Contrast in the microphotographs of the $PARP^{-/-}$ tissue was adjusted to allow visualization of tissue in the complete absence of staining. Microphotographs were taken with a ×630 objective with a cooled CCD camera. Abbreviations: Co, contralateral; Ip, ipsilateral; WT, wild type. Data shown are representative of duplicate experiments with either a monoclonal antibody or polyclonal antibodies.

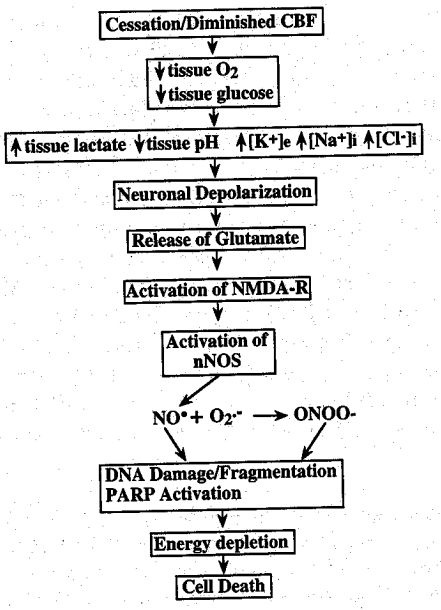

Fig. 7 A simple model of PARP activation in ischemia. Blood vessel occlusion induces a multitude of cellular events. PARP activation leading to cell death would fit into the known schema as follows: Ischemic events result in the reduction of the resting membrane potential of glia and neurons in the brain. Potassium leaks out of cells and depolarizes neurons leading to a massive release of glutamate. Acting via NMDA receptors, glutamate triggers a release of NO, which combines with superoxide to form peroxynitrite. Peroxynitrite damages DNA, and the fragments activate PARP. Massive activation of PARP leads to ADP-ribosylation and depletion of NAD. ATP is depleted in an effort to resynthesize NAD, leading to cell death by energy depletion.

anaerobic chamber for 60 min containing the gas mixture, 5% H_2/85% N_2/5% CO_2, maintained at 37 °C. Combined oxygen-glucose deprivation was terminated by removal of the cultures from the chamber and replacement of the EBSS solution with oxygenated growth medium. The cultures were returned to a humidified incubator containing 5% CO_2 and atmospheric oxygen at 37 °C overnight.

Toxicity was assayed 20–24 h after exposure to cytotoxic conditions by microscopic examination with computer-assisted cell counting following staining of all nuclei with 1 μg/ml Hoescht 33342 stain and staining of dead cell nuclei with 7 μM propidium iodide. Total and dead cells were counted. Glial nuclei fluoresce at a different intensity then neuronal nuclei and were gated out. Percent cell death was determined as the ratio of live-to-dead cells as compared with the percent cell death in control wells to account for cell death due to mechanical stimulation of the cultures. At least two separate experiments utilizing four separate wells were performed with a minimum of 15,000–20,000 neurons counted per data point. All reagents were purchased from Sigma Chemical Co.

Western blot analysis for PARP. For western blot analysis, fresh mouse brain was homogenized in 20% (wt/vol) 50 mM Tris-HCl (pH 7.4) buffer containing 1 mM EDTA, 1 mM dithiothreitol, 50 mM NaCl, 0.25 M sucrose, 0.2 mM PMSF and 1 mg/ml of chymostatin, leupeptin and pepstatin. The homogenate was centrifuged at 1000*g* for 15 min at 4 °C. The pellet, containing the nuclear fraction, was then washed with the homogenizing buffer. The nuclear fraction was dissolved in SDS–PAGE sample buffer containing 4 M urea. The mixture was subjected to an extensive sonication, followed by boiling at 90 °C for 15 min. The PARP protein (200 μg) was separated on a gradient SDS–PAGE and identified by anti-PARP monoclonal antibody by the enhanced chemiluminescence (ECL) method (Amersham, Arlington Heights, IL).

PARP catalytic assay. PARP activity was assessed using a method previously described[17]. Briefly, fresh mouse brain tissues were homogenized in 20% (wt/vol) 50 mM Tris-HCl (pH 7.4) buffer containing 1 mM EDTA, 1 mM dithiothreitol, 50 mM NaCl, 0.25 M sucrose, 0.2 mM PMSF and 1 μg/ml of chymostatin, leupeptin and pepstatin. The homogenate was centrifuged at 1000*g* for 15 min at 4 °C. The nuclear fraction, referred to as the pellet, was then washed with the homogenizing buffer. The washed pellet was resuspended in the homogenizing buffer. In a typical PARP assay, each 50 μl mixture contained 0.1 mM [adenylate-^{32}P]NAD (10 Ci/mmol) (NEN Life Sciences, Boston, MA). Following a 5-min incubation at 25 °C, 25 μl of 50% ice-cold TCA was added to each mixture, and the mixture was centrifuged at 8000*g* for 5 min. The resulting pellet was subjected to two more washes of 50% TCA and two washes of ice-cold acetone. After a brief air-drying, the pellet was dissolved in SDS–PAGE sample buffer containing 4 M urea and was boiled at 90 °C for 15 min. The PARP protein was separated on an 8% SDS–PAGE. The gel was fixed, dried and exposed to a PhosphorImager cassette (Molecular Dynamics, Sunnyvale, CA).

Ischemic model. The study was conducted in accordance with National Institutes of Health guidelines for the use of experimental animals, and the protocols were approved by the Institutional Animal Care and Use Committee. Adult male, 129/SV mice (Taconic Farms, Germantown, NY) or mutant *PARP* mice weighing 23–38 g were anesthetized with 1–1.2% halothane in oxygen-enriched air by face mask. The femoral artery was cannulated for measurement of arterial blood gases and blood pressure. Rectal temperature was controlled at or near 37 °C throughout the experiment with heating lamps/water pads in all animals. After baseline arterial blood gas measurement, unilateral MCAo occlusion was performed using intraluminal filament insertion with a 5-0 nylon monofilament. The filament was introduced into the internal carotid artery via the external carotid artery up to a point 6-mm distal to the internal carotid artery–pterygopalatine artery bifurcation. Concurrently, the ipsilateral common carotid artery was occluded by a temporary clip. After 2 h of ischemia, animals were briefly reanesthetized with halothane, and the filament was withdrawn through the external carotid artery, allowing reperfusion of the common and internal carotid arteries but not the external carotid artery.

Determination of infarction volume. After 2 h of ischemia and 22 h of reperfusion, brains were harvested for damage assessment. The forebrain was sliced into five coronal sections, 2 mm thick. These sections were stained with 1% 2,3,5-triphenyltetrazolium, as described[46]. Infarction volume was determined by numeric integration of areas of distinct pallor × section thickness using digital planimetry.

Immunohistochemical staining for poly(ADP-ribose) polymers. After 2 h of ischemia and 2 h of reperfusion, brains were rapidly removed and flash-frozen. To detect poly(ADP-ribose) polymerase activation, 15-μm-thick sections from fresh frozen brains were incubated in 200 μM NAD at 37 °C for 45 min with modifications[47]. Briefly, sections were fixed in 95% ethanol at 20 °C for 10 min and incubated overnight with mouse anti-poly (ADP-ribose) monoclonal antibody (Biomol Research Laboratories, Plymouth Meeting, PA) at a 1:100 dilution. A biotin-SP-conjugated goat anti-mouse IgG, F(ab')$_2$ specific antibody (Jackson ImmunoResearch Laboratories, West Grove, PA) was used as secondary at a 1:100 dilution. For signal amplification, an immunoperoxidase ABC kit (Vector Laboratories, Burlingame, CA) was used followed by a TSA-Indirect kit (NEN Life Sciences). Diaminobenzidine was used as a chromogen (Gibco BRL).

Acknowledgments

M.J.L.E. is supported by the Gustavus and Louise Pfeiffer Stipend. V.L.D. is supported by grants from the US Public Health Service (USPHS) NS33142 and the American Heart Association. T.M.D. is an Established Investigator of the American Heart Association and is supported by grants from the USPHS NS01578, NS33277 and the Paul Beeson Physician Scholars in Aging Research Program. P.D.H. is supported by grants from USPHS NIH NS33668, NR 03521 AND NS20020. R.J.T. is supported by USPHS NIH NS20020. J.B. is supported by NRSA NS09951. S.H.S. is supported by USPHS MH 18501 and Research Scientist Award DA-00074. Under an agreement between the Johns Hopkins University and Guilford, S.H.S., T.M.D. and V.L.D. are entitled to a share of sales royalties received by the University from Guilford. The University owns stock in Guilford, with S.H.S. and T.M.D. having an interest in the University share under University policy. S.H.S. serves on the Board of Directors

and the Scientific Advisory Board of Guilford, he is a consultant to the company, and he owns additional equity in Guilford. This arrangement is being managed by the Johns Hopkins University in accordance with its conflict-of-interest policies.

RECEIVED 27 JUNE; ACCEPTED 17 JULY 1997

1. Berger, N.A. Poly(ADP-ribose) in the cellular response to DNA damage. *Radiat. Res.* **101**, 4–15 (1985).
2. Lautier, D., Lagueux, J., Thibodeau, J., Menard, L. & Poirier, G.G. Molecular and biochemical features of poly(ADP-ribose) metabolism. *Mol. Cell. Biochem.* **122**, 171–193 (1993).
3. de Murcia, G. *et al.* Structure and function of poly(ADP-ribose) polymerase. *Mol. Cell. Biochem.* **138**, 15–24 (1994).
4. Althaus, F.R. & Richter, C. ADP-ribosylation of proteins: Enzymology and biological significance. *Mol. Biol. Biochem. Biophys.* **37**, 1–237 (1987).
5. de Murcia, G. & Menissier de Murcia, J. Poly(ADP-ribose) polymerase: A molecular nick-sensor. *Trends Biochem. Sci.* **19**, 172–176 (1994).
6. Lipton, S.A. & Rosenberg, P.A. Excitatory amino acids as a final common pathway for neurologic disorders. *N. Engl. J. Med.* **330**, 613–622 (1994).
7. Meldrum, B. & Garthwaite, J. Excitatory amino acid neurotoxicity and neurodegenerative disease. *Trends Pharmacol. Sci.* **11**, 379–387 (1990).
8. Choi, D.W. Glutamate neurotoxicity and diseases of the nervous system. *Neuron* **1**, 623–634 (1988).
9. Dawson, T.M. & Dawson, V.L. Protection of the brain from ischemia. in *Cerebrovascular Disease* (ed. Batjer, H.H.) 319–325 (Lippincott-Raven, Philadelphia, 1997).
10. Dawson, V.L., Dawson, T.M., London, E.D., Bredt, D.S. & Snyder, S.H. Nitric oxide mediates glutamate neurotoxicity in primary cortical cultures. *Proc. Natl. Acad. Sci. USA* **88**, 6368–6371 (1991).
11. Dawson, V.L., Dawson, T.M., Bartley, D.A., Uhl, G.R. & Snyder, S.H. Mechanisms of nitric oxide-mediated neurotoxicity in primary brain cultures. *J. Neurosci.* **13**, 2651–2661 (1993).
12. Dawson, V.L., Kizushi, V.M., Huang, P.L., Snyder, S.H. & Dawson, T.M. Resistance to neurotoxicity in cortical cultures from neuronal nitric oxide synthase deficient mice. *J. Neurosci.* **16**, 2479–2487 (1996).
13. Iadecola, C. Bright and dark sides of nitric oxide in ischemic brain injury. *Trends Neurosci.* **20**, 132–139 (1997).
14. Huang, Z. *et al.* Effects of cerebral ischemia in mice deficient in neuronal nitric oxide synthase. *Science* **265**, 1883–1885 (1994).
15. Beckman, J.S. & Crow, J.P. Pathological implications of nitric oxide, superoxide and peroxynitrite formation. *Biochem. Soc. Trans.* **21**, 330–334 (1993).
16. Radons, J. *et al.* Nitric oxide toxicity in islet cells involves poly(ADP-ribose) polymerase activation and concomitant NAD^+ depletion. *Biochem. Biophys. Res. Commun.* **199**, 1270–1277 (1994).
17. Zhang, J., Dawson, V.L., Dawson, T.M. & Snyder, S.H. Nitric oxide activation of poly(ADP-ribose) synthetase in neurotoxicity. *Science* **263**, 687–689 (1994).
18. Zhang, J., Pieper, A. & Snyder, S.H. Poly(ADP-ribose) synthetase activation: An early indicator of neurotoxic DNA damage. *J. Neurochem.* **65**, 1411–1414 (1995).
19. Wang, Z.-Q. *et al.* Mice lacking ADPRT and poly(ADP-ribosyl)ation develop normally but are susceptible to skin disease. *Genes Dev.* **9**, 509–520 (1995).
20. Suto, M.J., Turner, W.R., Arundel-Suto, C.M., Werbel, L.M. & Sebolt-Leopold, J.S. Dihydroisoquinolinones: The design and synthesis of a new series of potent inhibitors of poly(ADP-ribose) polymerase. *Anticancer Drug Des.* **6**, 107–117 (1991).
21. Banasik, M., Komura, H., Shimoyama, M. & Ueda, K. Specific inhibitors of poly(ADP-ribose) synthetase and mono(ADP-ribosyl)transferase. *J. Biol. Chem.* **267**, 1569–1575 (1992).
22. Banasik, M. & Ueda, K. Inhibitors and activators of ADP-ribosylation reactions. *Mol. Cell. Biochem.* **138**, 185–197 (1994).
23. Wang, Z.-Q. *et al.* PARP is important for genomic stability but dispensable in apoptosis. *Genes Dev.* (in the press).
24. Chan, P.H., Chu, L., Chen, S.F., Carlson, E.J. & Epstein, C.J. Reduced neurotoxicity in transgenic mice overexpressing human copper-zinc-superoxide dismutase. *Stroke* **21** (Suppl.), III80–III82 (1990).
25. Choi, D.W. Cerebral hypoxia: Some new approaches and unanswered questions. *J. Neurosci.* **10**, 2493–2501 (1990).
26. Dawson, T.M. & Snyder, S.H. Gases as biological messengers: Nitric oxide and carbon monoxide in the brain. *J. Neurosci.* **14**, 5147–5159 (1994).
27. Sharkey, J. & Butcher, S.P. Immunophilins mediate the neuroprotective effects of FK506 in focal cerebral ischaemia. *Nature* **371**, 336–339 (1994).
28. Kinouchi, H. *et al.* Attenuation of focal cerebral ischemic injury in transgenic mice overexpressing CuZn superoxide dismutase. *Proc. Natl. Acad. Sci. USA* **88**, 11158–11162 (1991).
29. Yang, G. *et al.* Human copper-zinc superoxide dismutase transgenic mice are highly resistant to reperfusion injury after focal cerebral ischemia. *Stroke* **25**, 165–170 (1994).
30. Endres, M., Wang, Z.-Q., Namura, S., Waeber, C. & Moskowitz, M.A. Ischemic brain injury is mediated by the activation of poly(ADP-ribose) polymerase. *J. Cereb. Blood Flow Metab.* (in the press).
31. Simpson, E.M. *et al.* Genetic variation among 129 substrains and its importance for targeted mutagenesis in mice. *Nature Genet.* **16**, 19–27 (1997).
32. Takahashi, K., Greenberg, J.H., Jackson, P., Maclin, K. & Zhang, J. Effect of inhibition of poly(ADP-ribose) synthetase on focal cerebral ischemia in rats. *Neurosci. Abstr.* (in the press).
33. Mizumoto, K., Glascott, P.A., Jr. & Farber, J.L. Roles for oxidative stress and poly(ADP-ribosyl)ation in the killing of cultured hepatocytes by methyl methanesulfonate. *Biochem. Pharmacol.* **46**, 1811–1818 (1993).
34. Heller, B. *et al.* Inactivation of the poly(ADP-ribose) polymerase gene affects oxygen radical and nitric oxide toxicity in islet cells. *J. Biol. Chem.* **270**, 11176–11180 (1995).
35. Thiemermann, C., Bowes, J., Myint, F.P. & Vane, J.R. Inhibition of the activity of poly(ADP ribose) synthetase reduces ischemia-reperfusion injury in the heart and skeletal muscle. *Proc. Natl. Acad. Sci. USA* **94**, 679–683 (1997).
36. Thies, R.L. & Autor, A.P. Reactive oxygen injury to cultured pulmonary artery endothelial cells: mediation by poly(ADP-ribose) polymerase activation causing NAD depletion and altered energy balance. *Arch. Biochem. Biophys.* **286**, 353–363 (1991).
37. Hudak, B.B., Tufariello, J., Sokolowski, J., Maloney, C. & Holm, B.A. Inhibition of poly(ADP-ribose) polymerase preserves surfactant synthesis after hydrogen peroxide exposure. *Am. J. Physiol.* **269**, L59–L64 (1995).
38. Kirkland, J.B. Lipid peroxidation, protein thiol oxidation and DNA damage in hydrogen peroxide-induced injury to endothelial cells: Role of activation of poly(ADP-ribose)polymerase. *Biochim. Biophys. Acta* **1092**, 319–325 (1991).
39. Said, S.I., Berisha, H.I. & Pakbaz, H. Excitotoxicity in the lung: *N*-Methyl-D-aspartate-induced, nitric oxide-dependent, pulmonary edema is attenuated by vasoactive intestinal peptide and by inhibitors of poly(ADP-ribose) polymerase. *Proc. Natl. Acad. Sci. USA* **93**, 4688–4692 (1996).
40. Szabo, C., Zingarelli, B., O'Connor, M. & Salzman, A.L. DNA strand breakage, activation of poly(ADP-ribose) synthetase, and cellular energy depletion are involved in the cytotoxicity of macrophages and smooth muscle cells exposed to peroxynitrite. *Proc. Natl. Acad. Sci. USA* **93**, 1753–1758 (1996).
41. Szabo, C., Saunders, C., O'Connor, M. & Salzman, A.L. Peroxynitrite causes energy depletion and increases permeability via activation of poly(ADP-ribose) synthetase in pulmonary epithelial cells. *Am. J. Respir. Cell. Mol. Biol.* **16**, 105–109 (1997).
42. Dawson, T.M., Bredt, D.S., Fotuhi, M., Hwang, P.M. & Snyder, S.H. Nitric oxide synthase and neuronal NADPH diaphorase are identical in brain and peripheral tissues. *Proc. Natl. Acad. Sci. USA* **88**, 7797–7801 (1991).
43. Bredt, D.S. *et al.* Nitric oxide synthase protein and mRNA are discretely localized in neuronal populations of the mammalian CNS together with NADPH diaphorase. *Neuron* **7**, 615–624 (1991).
44. Kaku, D.A., Goldberg, M.P. & Choi, D.W. Antagonism of non-NMDA receptors augments the neuroprotective effect of NMDA receptor blockade in cortical cultures subjected to prolonged deprivation of oxygen and glucose. *Brain Res.* **554**, 344–337 (1991).
45. Monyer, H. *et al.* Oxygen or glucose deprivation-induced neuronal injury in cortical cell cultures is reduced by tetanus toxin. *Neuron* **8**, 967–973 (1992).
46. Bederson, J.B. *et al.* Evaluation of 2,3,5-triphenyltetrazolium chloride as a stain for detection and quantification of experimental cerebral infarction in rats. *Stroke* **17**, 1304–1308 (1986).
47. Kupper, J.H., van Gool, L., Muller, M. & Burkle, A. Detection of poly(ADP-ribose) polymerase and its reaction product poly(ADP-ribose) by immunocytochemistry. *Histochem. J.* **28**, 391–395 (1996).

a

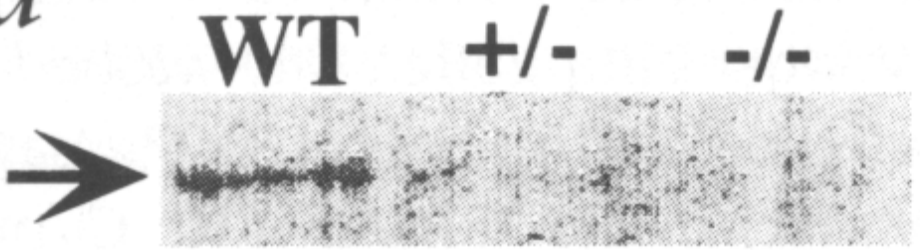

b

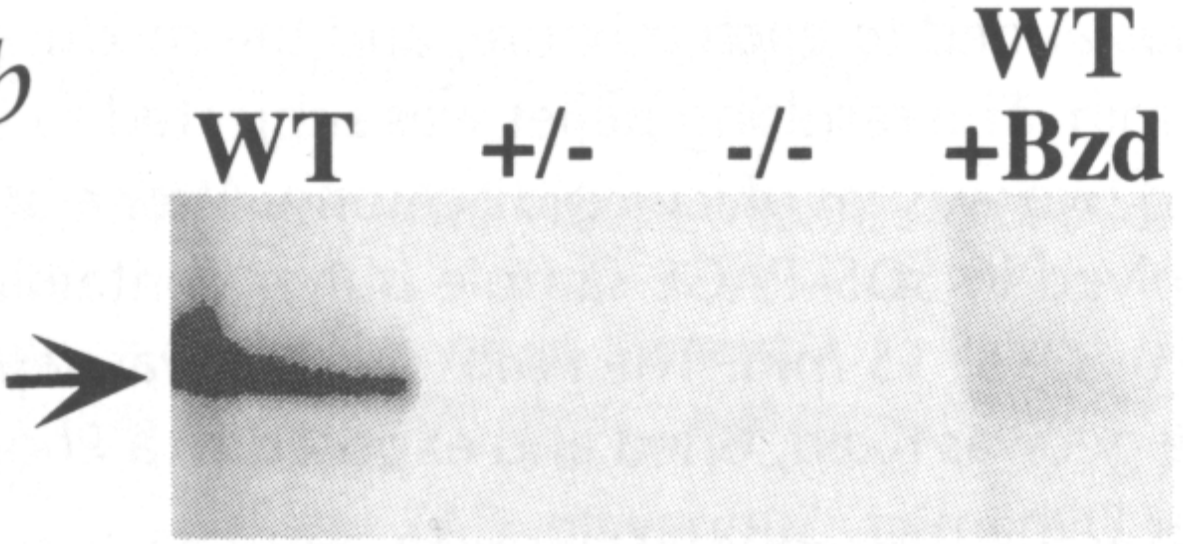

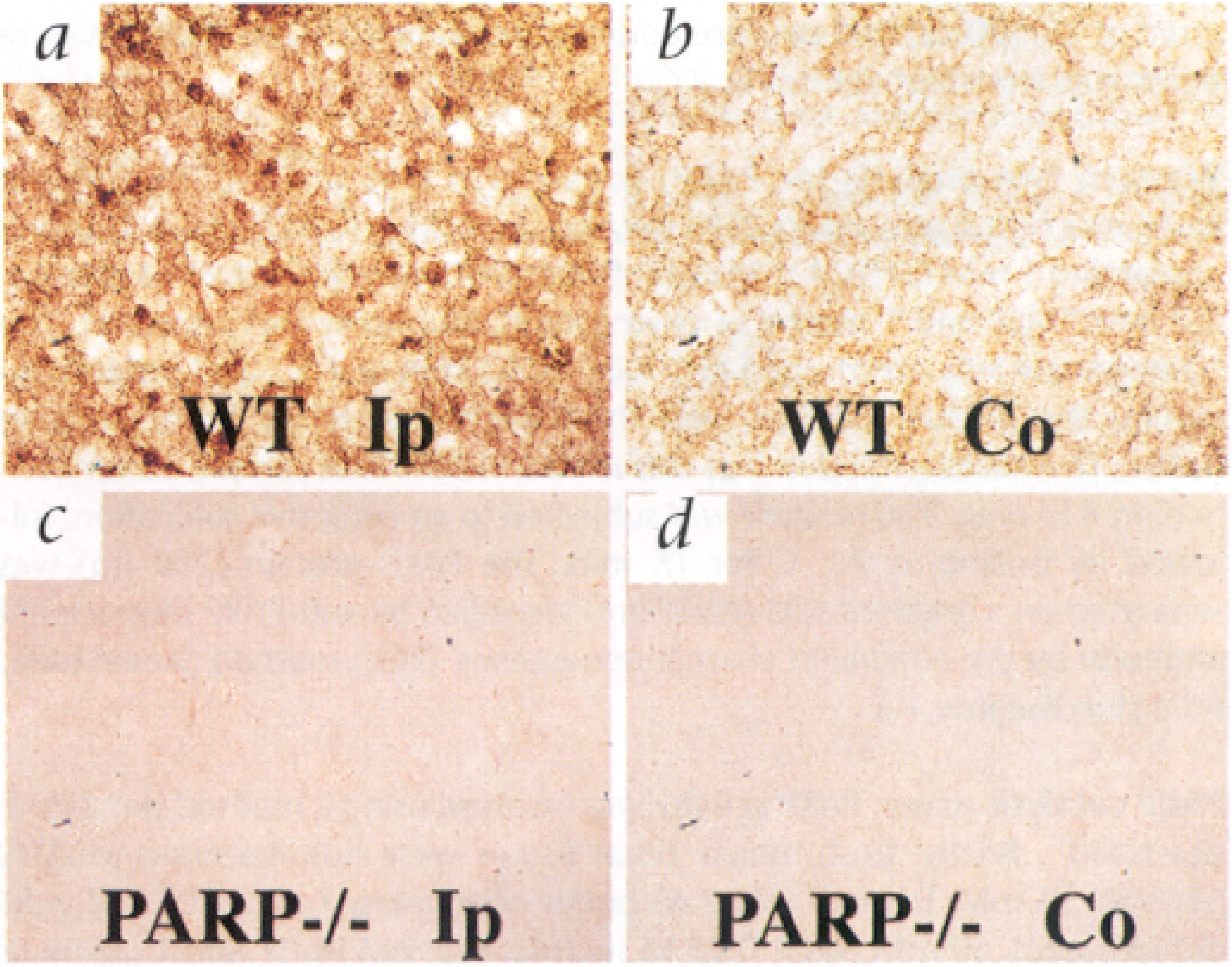
a
WT Ip
b
WT Co
c
PARP-/- Ip
d
PARP-/- Co